JOURNAL OF Materials CHEMISTRY

Oxidation mechanism of cobalt hydroxide to cobalt oxyhydroxide

V. Pralong, A. Delahaye-Vidal,* B. Beaudoin, B. Gérand and J-M. Tarascon

Laboratoire de Réactivité et de Chimie des Solides, Université de Picardie Jules Verne, UPRES-A 6007, 80039 Amiens Cedex, France. E-mail: Agnes.Delahaye@sc.u-picardie.fr

Received 5th October 1998, Accepted 27th January 1999

Although cobalt hydroxide is currently added to $Ni(OH)_2$ paste to prepare nickel composite electrodes used in Ni-based rechargeable alkaline batteries, its redox chemistry in alkaline media is still poorly documented. The $Co(OH)_2 \rightarrow CoOOH$ oxidation reaction in KOH media was investigated, and found to be dependent upon the experimental conditions, namely, temperature, oxidizing agent and reaction time. In addition, this reaction was shown, as determined by means of X-ray diffraction, electronic microscopy and atomic absorption measurements, to occur through a two step mechanism process involving first a dissolution process followed by a solid state reaction. This dissolution step enables preparation, by adjusting the cycling conditions, of cobalt oxyhydroxide with well defined morphology and texture, thereby providing an opportunity to optimize its efficiency as an additive in nickel electrodes.

Introduction

Cobalt hydroxide is currently used as an additive to nickel oxide electrodes (NOE) because of numerous beneficial effects on the electrode performance. Among the most important are (1) an enhancement of the nickel electrode conductivity,[1,2] (2) a better chargeability by raising the oxygen overpotential and/or lowering the NOE working electrode potential,[3,4] (3) a minimization of the γ-NiOOH growth at the NOE electrode during charging,[5] and (4) an increase in the NOE mechanical resistance.[6] Cobalt incorporation to the active mass (*e.g.*, NOE electrode) is usually realized either by chemical substitution of nickel during the $Ni(OH)_2$ synthesis (*e.g.*, co-precipitation) or by separate addition of a cobalted component, *i.e.* cobalt-based salts. When cobalt is co-precipitated with nickel into the active mass [*e.g.*, $Ni_{1-x}Co_x(OH)_2$], the cells display a maximum capacity for a cobalt content of 11 mol%.[7]

By contrast, when cobalted additives such as cobalt hydroxide or cobalt monoxide are used, the enhanced NOE electrode capacity is believed[1] to be due to the presence of a high conducting phase formed by oxidation of the cobalted precursor. According to Oshitani *et al.*,[1] the divalent cobalt-based precursor dissolves in the electrolyte forming a deep blue complex, and then CoOOH reprecipitates around the platelets of the nickel hydroxide, leading to a good electrical pathway between them. However, starting from the $Co(OH)_2$ precursor, the dissolution step is not fully demonstrated. Soubirous[8] has studied the $Co(OH)_2 \rightarrow CoOOH$ transformation in various media by electron microscopy analyses. When the reaction was conducted in alkaline medium, it was reported that the shapes of the CoOOH particles completely differed from those of the $Co(OH)_2$ precursor, suggesting a dissolution–recrystallization process. By contrast, when the oxidation of divalent cobalt was conducted in water at 80 °C under an oxygen pressure of 5 bar, a strong textural relationship between the starting $Co(OH)_2$ phase and the oxidation product was noted, implying the predominance of a solid state reaction mechanism over the dissolution–recrystallization process. Finally, through other studies,[9–11] the temperature was also found to influence both the kinetics and textural changes involved during the $Co(OH)_2 \rightarrow CoOOH$ transformation.

All the above results indicate that the oxidation $Co(OH)_2 \rightarrow CoOOH$ reaction path is strongly dependent upon the experimental conditions. Thus, the aim of this paper is to investigate the influence of other experimental parameters, in the $Co(OH)_2 \rightarrow CoOOH$ reaction mechanism in order to better understand how CoOOH forms in electrochemical cells. In our approach, the oxidation reaction was performed either by chemical or electrochemical routes in either water or concentrated KOH solution. From combined transmission electron microscopy, X-ray diffraction and atomic absorption analysis, depending on the experimental conditions, various reaction pathways are proposed for the $Co(OH)_2$/CoOOH transformation.

Experimental

Commercial cobalt hydroxide (UM Belgium) denoted as β(II) (crystallizing in the $P\bar{3}m1$ space group with $a = 3.1828$ Å and $c = 4.6537$ Å) was used for all the experiments; it consists of large monolithic platelets (400×2000 Å), showing Bragg extinction contours as determined by TEM observations.

The cobalt solubility, unless otherwise specified, was determined by placing 250 mg of commercial cobalt hydroxide in 250 ml of oxygen-free solution (either water or 5 M KOH). The suspension was placed at room temperature in an autoclave (Parr Instrument model 4842) under argon. Sample withdrawals were performed while the $Co(OH)_2 \rightarrow CoOOH$ reaction was in progress. The solid was separated from the solution by centrifugation prior to characterization by X-ray diffraction (XRD). The solution (sample surpernatant) was analyzed for Co content by atomic absorption (AA).

The electrochemical oxidation of $Co(OH)_2$ was carried out as follows: 65% of commercial cobalt hydroxide, 30% Super P carbon black (from M.M.M., Belgium) used as electronic binder, and 5% polytetrafluoroethylene (PTFE) used as mechanical binder were thoroughly mixed to form the active paste. The composite cobalt electrodes were prepared by inserting the above paste into a 2.25 mm thick nickel foam plate. These electrodes were dried at 50 °C and cut into disks (1.15 cm^2), which were then pressed at *ca.* 2 tonnes cm^{-2}. For the negative electrode, 1.15 cm^2 disks were directly cut from SAFT Cd/$Cd(OH)_2$ electrodes. Swagelok laboratory electrochemical test cells were made with the positive [$Co(OH)_2$] electrode separated from the Cd negative electrode by a polyamide separator impregnated with 5 M KOH solution. The electrochemical tests were carried out using an Arbin cycling system (Arbin Co., TX, USA) operating in galvanostatic mode, which can deliver currents up to 1 A with *ca.* 0.01% accuracy.

Chemical oxidation was performed according to three different methods.

(1) By reaction of the β(II) precursor phase with a given volume of NaClO (*ca.* 8 M) in the presence of 5 M KOH.

(2) By precipitation, in an autoclave under oxygen pressure, of cobalt oxyhydroxide from a deep blue solution obtained by dissolving cobalt monoxide (CoO) in 5 M KOH. The CoOOH precipitate was recovered from the solution by centrifugation.

(3) By oxidation, in a stainless steel autoclave under 20 bar oxygen pressure, of $Co(OH)_2$ powder dispersed in water or in 5 M KOH under stirring.

Diffraction patterns were collected using a Philips diffractometer PW1710 with Cu-Kα radiation ($\lambda = 1.5406$ Å). A Scanning Philips Field Effect Gun (FEG) microscope with a resolution of *ca.* 10 Å was used to study the macrotexture changes, while the sample morphologies were determined by means of a Philips transmission electron microscope (TEM) CM12 instrument. Finally, the cobalt species in solution were determined by atomic absorption spectrophotometry (Perkin Elmer 300).

Results

1 Solubility measurements

Cobalt hydroxide is known to be amphoteric and is soluble in both acidic and alkaline media. In an alkaline solution, cobalt hydroxide reacts to form the $Co(OH)_4^{2-}$ dicobaltite ion currently named 'deep blue'. In order to quantify the amount of complexed Co in the alkaline solution, we have studied the solubility of cobalt hydroxide in an autoclave under argon atmosphere and continuous stirring. The solubility was found to reach a limit of 48 mg L^{-1} after 12 h. From the evolution of the X-ray diffraction patterns of withdrawn samples (Fig. 1) during the course of the treatment, no structural change could be determined, with the exception of a relatively high background at high *d*-spacing. The $Co(OH)_2$ platelet-like morphology is mainly preserved during the reaction with, however, a subtle difference in the platelet contours that are more blurred for $Co(OH)_2$ powders treated for 48 h in 5 M KOH. Such a difference can be seen by TEM measurements [Fig. 2(b)], which reveal the growth of small crystallites around

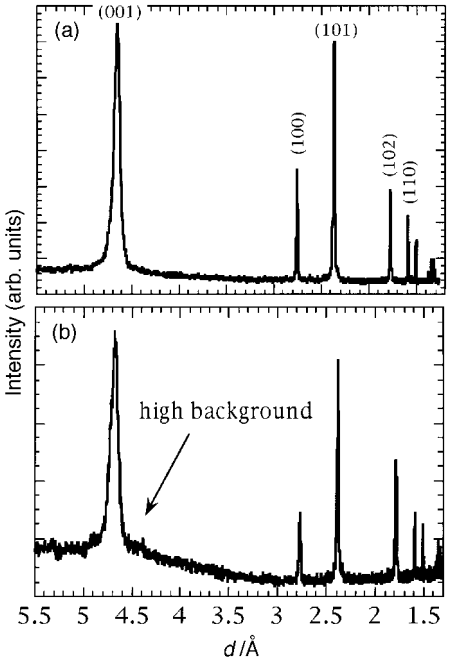

Fig. 1 X-Ray diffraction patterns of cobalt hydroxide in concentrated KOH under an atmosphere of argon. (a) Commercial $Co(OH)_2$ and (b) the product obtained after 48 h in alkaline solution under argon atmosphere.

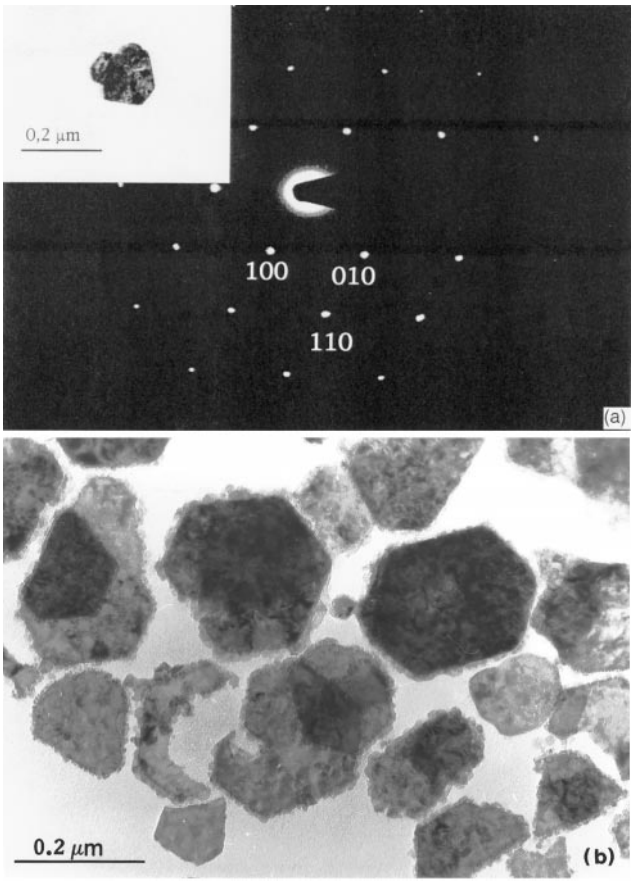

Fig. 2 (a) TEM micrographs from commercial cobalt hydroxide (UM Belgium). (i) Particles lying on the (001) plane with Bragg extinction contours. (ii) SAED of the same particle showing sharp electron diffraction spots indicating good crystallinity. (b) Transmission electron microscopy image of the cobalt hydroxide after standing in alkaline suspension under argon atmosphere. The Bragg extinction contours observed inside the particles indicate good crystallinity of the platelets. On the edge of platelets, very small nuclei appear.

the $Co(OH)_2$ platelets. These crystallites could correspond to CoOOH, resulting from the oxidation of $Co(OH)_2$, as suggested by the color change of the solution from pink to beige during the reaction. These observations imply that CoOOH reprecipitates from cobalt species present in the solution, consistent with the well known stability of Co^{3+} in KOH solution. These very small CoOOH crystallites, the dimensions of which are below the coherence length of the X-rays, could also explain the enhanced diffuse scattering observed underneath the main $Co(OH)_2$ Bragg peaks in Fig. 1. While well experimentally evidenced, it is intriguing that the oxidation reaction takes places when the experiments are conducted under argon atmosphere. A possibility that we cannot totally eliminate is that the oxidation actually proceeds when samples are in contact in air prior to their characterization.

Finally, the solubility of $Co(OH)_2$ in water after one week storage under argon was also checked. After this time, no Co was found (as determined by AA) in the washed solution implying that the cobalt hydroxide is not soluble in water. In addition, the morphology of $Co(OH)_2$ remains unchanged.

2 Electrochemical oxidation

A $Co(OH)_2$/Cd cell was charged at a C/10 rate over 20 h, dismantled, and the positive Co electrode recovered for X-ray characterization. The X-ray powder pattern of the final product was identical to that of β-CoOOH reported by Feitknecht,[12] and completely indexed in trigonal symmetry on the basis of a hexagonal cell (space group $R\bar{3}m$) with lattice parameters $a = 2{,}857$ Å and $c = 13{,}266$ Å. The charge–voltage

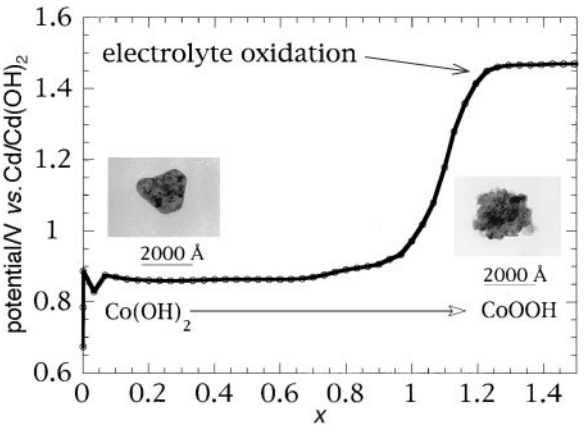

Fig. 3 Potential evolution of cobalt hydroxide during a first charge, and a bright field image of both the initial platelets and the electrochemically prepared CoOOH after a first charge (C/10, 20 h).

composition curve for the $Co(OH)_2$/Cd cell shows a well defined flat plateau at 0.86 V (Fig. 3) suggesting that the $Co(OH)_2 \rightarrow CoOOH$ oxidation reaction is biphasic. TEM measurements of a CoOOH particle obtained at the end of the first charge (Fig. 3) reveal that the general particle form has been retained with, however, the clear appearance of irregular contours. This type of transformation, where important changes in texture are observed while a memory effect links starting and final products, is often referred to as a metasomatic process.[13] Such transformations often take place when dissolved chemical species react on the external surface of a solid. In our experiments, the amount of cobalt in the 5 M KOH electrolyte was monitored as a function of time during the electrochemical oxidation. A cobalt content of 8 mg L^{-1} was detected at the beginning of the oxidation, and this Co content was found to progressively decrease during the charge down to a value of <1 mg L^{-1}. These low values are consistent with a metasomatic transformation but do not unambiguously imply a mechanism occurring *via* the solution.

At this point the legitimate question to ask deals with the interplay between the high cobalt solubility and the texture of the obtained CoOOH. Rather than pursuing such a microscopy study on electrochemically made Co-based electrodes containing several additives such as PTFE and carbon that could act as obstacles, we prefer to embark in a chemical simulation approach of the $Co(OH)_2 \rightarrow CoOOH$ oxidation reaction.

3 Chemical oxidation of $Co(OH)_2$

The XRD patterns of the powdered samples obtained after oxidation of $Co(OH)_2$ with NaClO display relatively broad Bragg peaks located at similar positions to those reported for the pure β-CoOOH phase. TEM micrographs indicate that the particles morphology does not change during the reaction [*cf.* Fig. 4(a) and 2(a)] *i.e.*, the reaction is pseudomorphous. From the presence of arched diffraction spots in the corresponding SAED pattern [Fig. 4(b)], a mosaic structure can directly be assigned to the β-CoOOH particles [also designated β(III)]: this means that a single particle contains several slightly disoriented coherent diffraction domains. The mosaicity of the grain is also confirmed by the dark field image. SAED patterns of partly transformed particles (not shown here) also indicate that the oxidized phase grew with a well defined and reproducible orientation with respect to the β(II) $Co(OH)_2$ precursor hydroxide phase (*i.e.* a topotactic reaction). Crystallographically speaking, the [001] and [110] axis directions of the β(II)-phase are parallel to the [003] and [110] directions of the β(III)-phase, respectively. This information, combined with the retention of the particle shape during the oxidation reaction implies that the reaction most

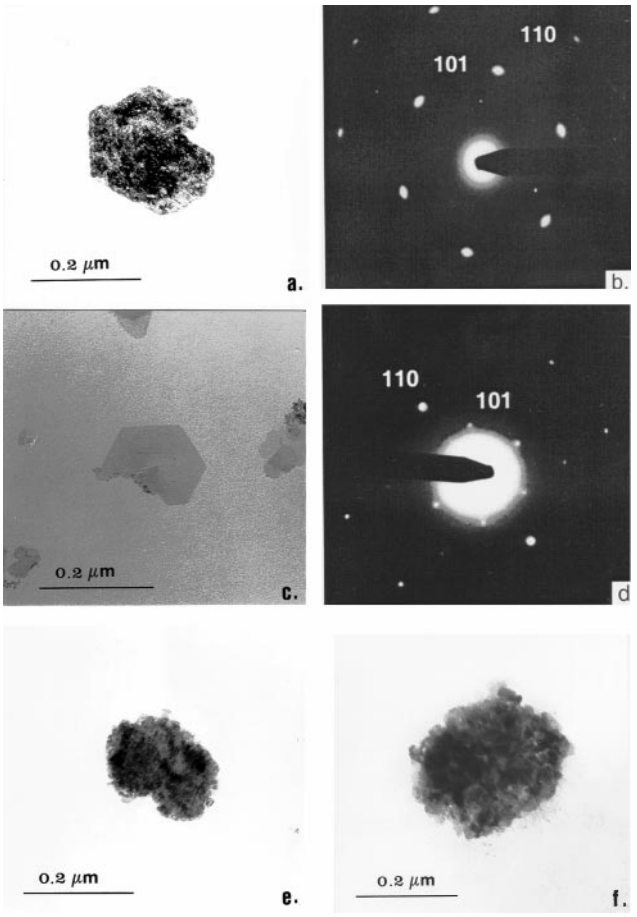

Fig. 4 β-CoOOH obtained by various oxidation routes; (a) and (b) bright field image of β-CoOOH prepared by NaClO oxidation and corresponding SAED of single platelet. The diffraction spots are broad arches showing a misorientation of the crystallites inside the particle; (c) and (d) Bright field image of a particle of β-CoOOH obtained by direct precipitation and SAED showing the particle lies on the (001) plane. The diffraction spots appear very sharp, characterizing a monolith texture. (e) Bright field image of cobalt oxyhydroxide prepared electrochemically. (f) Chemical oxidation under hydrothermal conditions (5 M KOH solution, 20 bar oxygen pressure).

likely occurs in the solid state by oriented growth of β(III) on β(II) in the (001) plane. The solid state growth then induces strains within the particles. These strains, due to the unit cell mismatch between the cobalt(II) and cobalt(III) phases, lead to the formation of a mosaic texture. Note that such a solid state mechanism is supported by our inability to detect any amount of cobalt in solution during the oxidation.

In short, the textural features of CoOOH prepared by oxidation with NaClO completely differ from those of electrochemically prepared CoOOH. In the latter case we observe, instead of a pseudomorphous reaction, a metasomatic reaction and, in addition, the growth of numerous CoOOH crystallites around the particle edge.

For the cobalt oxyhydroxide samples prepared in alkaline media by direct precipitation under oxygen pressure the starting solution contained 150 mg L^{-1} of $Co(OH)_4^{2-}$ obtained by dissolution of cobalt monoxide (CoO) in concentrated alkaline medium (8.5 M KOH). After 24 h the precipitation reaction was complete and the solid was separated from the solution by centrifugation. No trace of Co was detected in the washed solution by AA analysis. The X-ray diffraction pattern of the recovered solid was identical to that of CoOOH obtained by oxidation with NaClO. The bright field image of the final product presents pseudo-hexagonal platelets [Fig. 4(c)], and the selected area electron diffraction (SAED) pattern of an isolated grain corresponds to a single crystal lying on (001)

plane [Fig. 4(d)]. The sharpness of the electron diffraction spots indicate that the platelets of this CoOOH phase may be considered as monolithic single crystals (*i.e.* each platelet consists of a unique coherent diffraction domain). In this case, the precursor suspension was a KOH solution containing cobalt complexes $Co(OH)_4^{2-}$ from which formation of the most stable phase in alkaline suspension, *i.e.* β-CoOOH, is expected to occur.

The final CoOOH synthesis method consists of the transformation of cobalt hydroxide to oxide hydroxide under an oxygen atmosphere of 20 bar. From AA analysis which indicates no Co dissolution, and X-ray diffraction measurements combined with microscopy studies, we conclude that the $Co(OH)_2 \rightarrow$CoOOH oxidation reaction is not possible in water. Even after two weeks the final product retained its typical pink color. These results further stress that the dissolution of cobalt hydroxide is a major element in the oxidation process. By switching from water to 5 M KOH the results are totally different.

Attempts to prepare CoOOH from $Co(OH)_2$ in KOH media under oxygen pressure were first conducted at room temperature for 24 h. The resulting samples were characterized as above. A comparison [Fig. 4(e) and (f)] between the macrotexture of hydrothermal CoOOH and that of electrochemically prepared CoOOH suggests that the $Co(OH)_2 \rightarrow$CoOOH oxidation proceeds similarly in both cases, leading to hexagonal CoOOH with irregular contours and with a completely different internal texture that is now highly porous and granular. The X-ray diffraction patterns (Fig. 5) of the withdrawn products during the course of the experiment reveal a biphasic reaction, with the final product being the β-CoOOH cobalt oxyhydroxide phase as for the electrochemical oxidation. Study by SEM and TEM of samples recovered during the course of the reaction allows a better understanding of the progress of the reaction.

Micrographs show that at the start of the reaction the edges of the platelets become uneven with reduced and enlarged parts [Fig. 6(a) and (b)], suggesting that part of the starting material is dissolved, and then reprecipitated both around the edge and at the grain boundaries. SAED measurements (not shown here) on the external part of the partly transformed

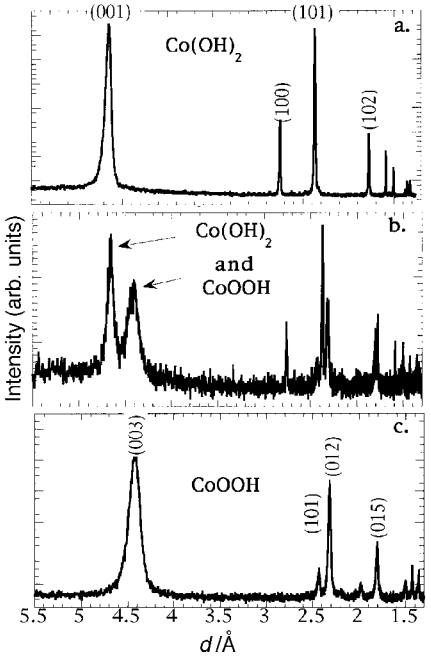

Fig. 5 X-Ray diffraction pattern evolution of β-$Co(OH)_2$ in alkaline solution under hydrothermal conditions. (a) Platelets of $Co(OH)_2$, (b) intermediate sample and (c) final platelets of CoOOH.

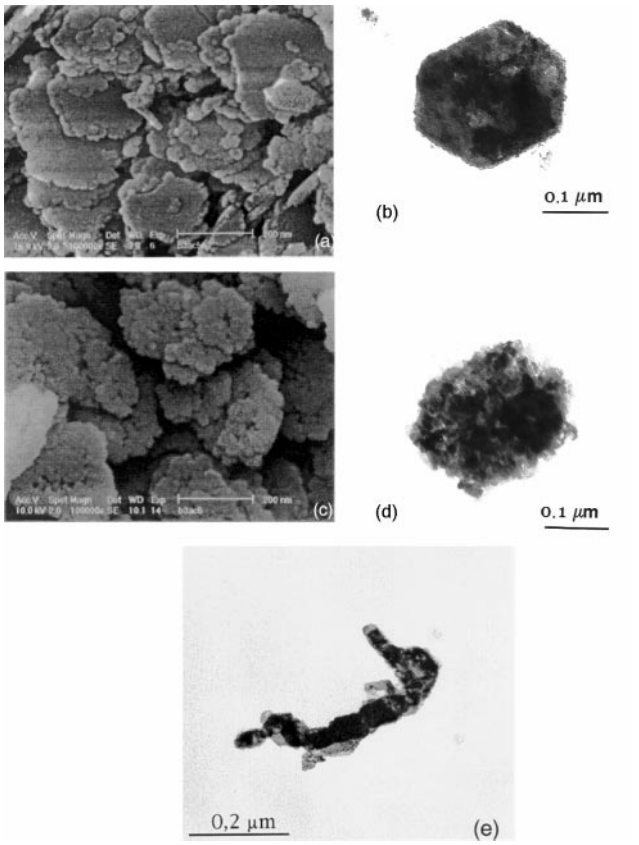

Fig. 6 SEM and TEM study of β-$Co(OH)_2$ transformation in alkaline solution under oxygen atmosphere: (a, b) beginning of the reaction, (c, d) platelets during the oxidation in an advanced state and (e) final platelets of β-CoOOH after desaggregation.

platelet indicated that the resulting β(III) crystallites located at the edge or grain boundaries showed a definite reproducible orientation with respect to the precursor β(II) phase. The [110] direction is common to both β(II) and β(III) phases suggesting that nucleation (*e.g.*, oxidation reaction) proceeds along this crystallographic direction. During the following stage, the platelet cores also transform leading to a very porous internal mosaic texture [Fig. 6(c) and (d)]. Finally, by leaving the final product in the KOH suspension for 48 h, a partial disintegration of the CoOOH platelets was observed. TEM measurements of the final product shown in Fig. 6(e) reveal that the platelets, which have precipitated around the edges of the $Co(OH)_2$ platelets and in the grain boundaries stick together, therefore the coherence domains increase during the course of crystalline growth.

In short, under hydrothermal conditions, the $Co(OH)_2 \rightarrow$CoOOH oxidation reaction is initiated by a partial dissolution of $Co(OH)_2$ particles, leading to Co^{2+} ions which are then oxidized to Co^{3+} in solution, and nucleated as a CoOOH phase that grows on the residual $Co(OH)_2$ grain along a nucleation axis [110] common to both phases. Such a solution reaction path presents some difficulties in accounting for the observed platelet porosity that is usually ascribed to strain relaxation for a purely solid state reaction. Thus a remaining question is whether the final porous/granular texture could originate from the dissolution of the core particle, which should be favoured at higher temperatures. In order to test this hypothesis a similar experiment was conducted at 350 K rather than 298 K.

Raising the temperature increases the size of the external platelets resulting from the dissolution/germination/growing process described above. The bright and dark field images of a large platelet are shown in Fig. 7(a) and (b), respectively.

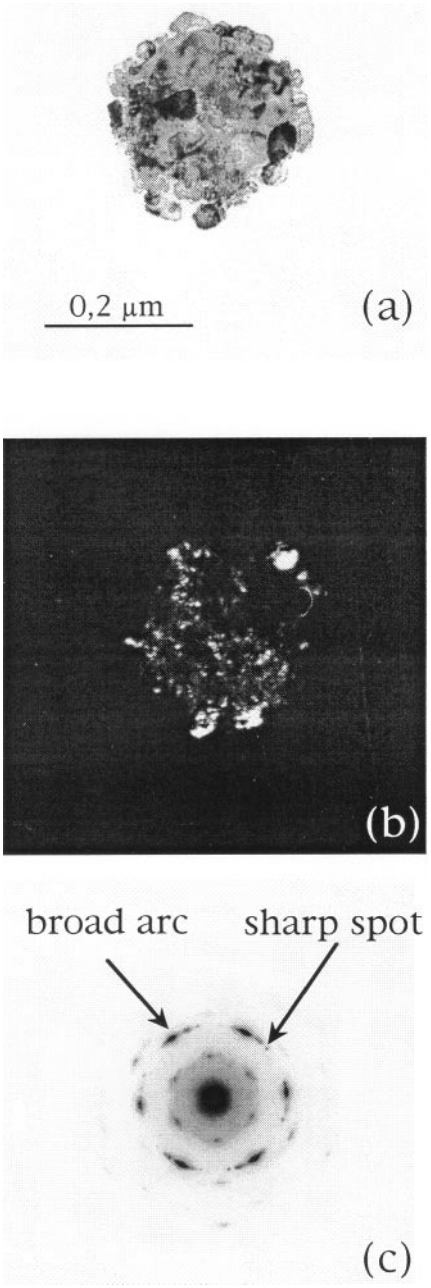

Fig. 7 Evidence of the two mechanisms during the oxidation at 50 °C in 5 M KOH. (a) Bright field image of a platelet at the beginning of the reaction. (b) Dark field image of the same platelet showing the mosaic texture of the grain inside the particle and the crystallites on the edge of the homogeneously illuminated particle, indicating that the crystallites on the edge are monolithic. (c) The SAED pattern is characterized by a set of rings with sharp spots and small arcs confirming the presence of both monolithic and mosaic texture.

Homogeneous illumination around the platelet edges is seen indicating that each crystallite visualized on the edge is monolithic. In contrast, the core of the initial platelets shows a large number of small white spots, the size of which are about the same order of magnitude as that of the mean crystallite size, indicating the core mosaic texture of these platelets. The presence of both monolithic and mosaic texture is confirmed by SAED [Fig. 7(c)]. This experiment indicates that core dissolution does not occur, but allows us to conclude that the dissolution/nucleation/growing process giving rise to the growth of small β-CoOOH monolithic particles on the platelet edges only takes place at the early stage of the oxidation process. Subsequently, the oxidation reaction is a solid state process proceeding from the edge to the core of the platelet,

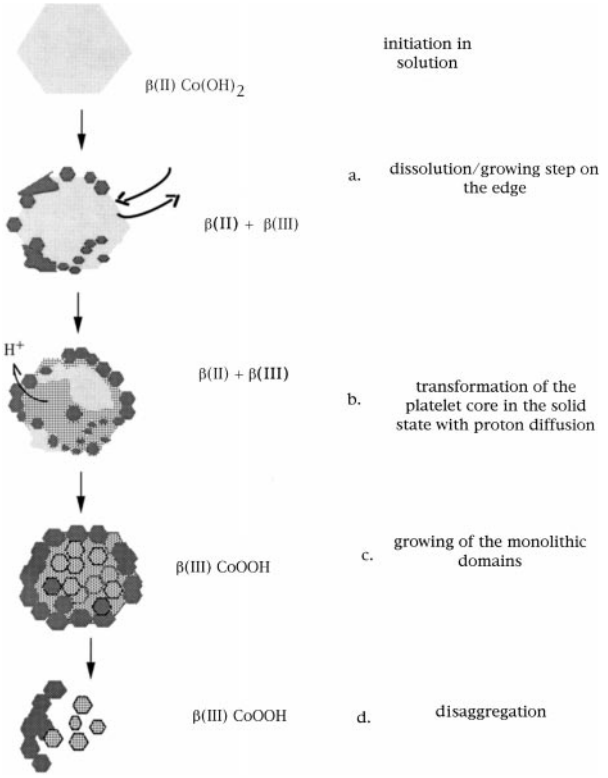

Fig. 8 Schematic mechanism of the cobalt hydroxide oxidation to cobalt oxyhydroxide under hydrothermal conditions (5 M KOH and 20 bar oxygen pressure).

and inducing strains within the particles that are released to form a highly porous particle having a mosaic texture.

Discussion

We have reported the electrochemical synthesis of CoOOH and compared its crystal chemical and textural aspects with those of chemically obtained CoOOH. Depending upon the oxidizing agent (NaClO or pressurized oxygen) the chemical oxidation reaction can follow two different pathways leading to cobalt oxyhydroxide with different textures. When a strong oxidizing agent such as NaClO is used there is no cobalt dissolution, and we are dealing with a pure solid state oxidation. In contrast, it is shown that when Co^{2+}-based complexes in KOH solution are used as precursors, a monolithic cobalt oxyhydroxide is obtained through a germination/growth process. Finally, when CoOOH is prepared by a hydrothermal route, the oxidation reaction appears to occur in two steps as schematically shown in Fig. 8. The first step is a dissolution and growth step [Fig. 8(a)], which depends on temperature. More specifically, nuclei of the CoOOH phase form on the external part and on grain boundaries of the partially dissolved particles, and then grow by feeding from the solution leading to monolithic domains. With increased temperature, this growth step is favoured. The second step gives rise to the transformation of the initial platelet core that occurs in the solid state, and involves a proton diffusion process [Fig. 8(b)]. During the reaction process, the strains create misfits, so the final product has an internal mosaic texture. Simultaneously, *via* intermediate species in solution, reorganization and mass transfer occur for the monolithic external domains leading to a pseudo-sintering effect [Fig. 8(c)]. At the end of the reaction, a disintegration of the small mosaic particles at the core of the initial platelets [Fig. 8(d)] is observed. Only monolithic particles from the dissolution process are large enough not to be affected by this disintegration process. This two-step mech-

anism implies the capability of favoring one reaction over another during electrochemical oxidation.

Conclusion

We have obtained direct experimental evidence that the cobalt hydroxide oxidation is a two-step reaction which can be fine tuned by varying the chemical or electrochemical conditions. For instance, increasing the temperature during chemical simulation favors the growth of monolithic oxyhydroxide. On another hand, using a strong oxidant agent such as NaClO induces solid state oxidation, which gives rise to a granular texture with conservation of the general shape. These findings provide a better appreciation of the importance of the cycling rate and temperature on the morphology/texture of the cobalt oxyhydroxide that mainly governs the electrochemical behavior. Such information is of substantial importance for the formation of the Ni-based cells containing $Co(OH)_2$ additives as will be reported in the future. Under the experimental conditions presently used we only observed the formation of CoOOH. However, it is quite conceivable for instance, that by prioritizing the nucleation/growing phenomena through the use of more severe experimental conditions (*e.g.* temperature), one could stabilize another phase. Studies have been undertaken along this direction, and preliminary results indicate in special cases[14] the formation of a Co_3O_4 phase at the expense of β-CoOOH.

Acknowledgements

The authors thank Y. Chabre for his enlightening discussions, and J.-B. Leriche for his technical assistance. They are grateful to the Union Minière (UM) for their financial support and enlightening discussions.

References

1 M. Oshitani, H. Yufu, K. Takashima, S. Tsuji and Y. Massumaru, *J. Electrochem. Soc.*, 1989, **136**, 1590.
2 L. Gautier, Thesis, University of Bordeaux I, 1995.
3 B. E. Ezhov and O. G. Malandrin, *J. Electrochem Soc.*, 1991, **138**, 885.
4 R. D. Armstrong and E. A. Charles, *J. Power Sources*, 1989, **25**, 89; D. H. Fritts, *J. Electrochem Soc.*, 1982, **129**, 118.
5 J. Mc Breen, W. E. O'Grady, G. Tourillon, E. Dartyge, A. Fontaine and K. I. Pandya, *J. Phys. Chem.*, 1989, **93**, 6308.
6 R. D. Armstrong, G. W. D. Briggs and E. A. Charles, *J. Appl. Electrochem.*, 1988, **18**, 215.
7 A. Audemer, A. Delahaye, R. Farhi, N. Sac-Epée and J-M. Tarascon, *J. Electrochem. Soc.*, 1997, **144**, 2614.
8 R. Soubirous, Thesis, University of Paris VII, 1970.
9 P. Benson, G. W. D. Briggs and W. F. K. Wynne-Jones, *Electrochim. Acta*, 1964, **9**, 275.
10 M. Figlarz, J. Guenot and J-N. Tournemolle, *J. Mater. Sci.*, 1974, **9**, 772.
11 M. Figlarz, J. Guenot and F. Fievet-Vincent, *J. Mater. Sci.* , 1976, **11**, 2267.
12 W. Feitknecht, *Bull. Soc. Chim. Fr.*, 1949, **5**, D-31.
13 J. Burkank, *J. Electrochem. Soc*., 1966, **113**, no. 9.
14 V. Pralong, A. Delahaye-Vidal, B. Beaudoin and J.-M. Tarason, *J. Electrochem. Soc.*, submitted.

Paper 8/07689H